RT&A, No 3 (79)
Volume 19, September 2024

A NOVEL ASYMMETRIC COMPOUND CLASS OF DISTRIBUTIONS WITH ESTIMATION AND APPLICATION

A.G. Al-Kilany[1], Amal S. Hassan[2*], L.S. Diab[3], and E.S. El-Atfy[1]

[1]Faculty of Science for (girls), Al-Azhar University, Nasr City, 11884, Egypt,

[2*]Faculty of Graduate Studies for Statistical Research, Cairo University, 12613, Giza, Egypt
amal52_soliman@cu.edu.eg

[3]Department of Mathematics and Statistics, Faculty of Science, Imam Mohammad Ibn Saud Islamic University (IMSIU), Riyadh 11432, Saudi Arabia

***Correspondence: Email** amal52_soliman@cu.edu.eg

Abstract

This paper introduces and discusses the novel asymmetric class of distributions that have the name inverse power Lomax power series (IPLPS). This class of distributions is produced by combining the inverse power Lomax with the power series distributions. This combined approach provides an opportunity for the creation of flexible distributions with significant physical implications in many fields, like biology and engineering. The IPLPS distributions encompass several new compound distributions as sub-models along with a new class of compound distributions. Many statistical features, including moments, quantile function, conditional moments, inverse moments, uncertainty measures, and probability-weighted moments, are obtained. As a special model of the generated class, the parameters of the inverse power Lomax Poisson distribution are estimated by different methods, including least squares, Cramér von Mises, maximum likelihood, and weighted least squares. Through an extensive simulation analysis, the execution of different parameter estimation techniques for the inverse power Lomax Poisson model is performed to show its validity based on its mean squared error and absolute bias. Two real datasets are utilized to show the practicality of the newly generated model. Results show that the inverse power Lomax Poisson distribution provides the most fitted model for these datasets in comparison to other distributions such as power Lomax, Marshall-Olkin power Lomax, power Lomax Poisson, and Topp-Leone Lomax distributions.

Keywords: Power series distributions, inverse power Lomax distribution, moments, compounding, Havrda and Charvat measure, Cramér von Mises.

1. Introduction

Recent academic focus has shifted towards the creation of new univariate distributions. Univariate distributions, whether for theoretical, practical, or combined purposes, hold significant importance in statistical and related fields. Analyzing the reliability of experimental failure components is a primary objective. It's often assumed that these failures occur due to certain processes, yet a thorough investigation into the causes of component failure seems lacking; see Barreto-Souza et al. [1]. Consider a system's lifetime composed of N components, and N is the discrete random variable that follows geometric, Poisson, logarithmic, or binomial distributions.

Power series (PS) is the general form of these chosen distributions. For further information on the PS class of distributions, refer to Noack [2]. Suppose that X denotes the continuous random variable for each component. Consequently, the random variable X= Min($X_1,X_2,\ldots,X_N$) or X= Max($X_1,X_2,\ldots,X_N$) signifies any component lifetimes depending on whether they are arranged in a series or in parallel structure, respectively.

Suppose that the random variable N associated with the PS class of distributions, characterized by a probability mass function, is given by:

$$P(N=n)=\frac{a_n\theta^n}{C(\theta)}, \qquad n=1,2,\ldots\ldots$$

where $a_n \geq 0$ only dependent on n, and $C(\theta)=\sum_{n=1}^{\infty} a_n\theta^n$ is finite.

Several compound lifetime models have been created by combining several lifetime distributions with the PS class of distributions. For instance, the exponential PS [3], the Weibull-PS [4], Lindley-PS [5], exponential Pareto-PS [6], Burr XII-PS [7], exponentiated power Lindley-PS [8], generalized Burr XII-PS [9], odd log-logistic-PS [10], Topp-Leone generalized exponential-PS [11], power function-PS [12], inverse gamma-PS [13], inverse exponentiated Lomax-PS [14], beta exponential-PS [15], unit exponentiated half logistic-PS [16], inverted Nadarajah-Haghighi-PS [17], power quasi Lindley-PS [18], unit Burr XII-PS [19], unit Gompertz-PS [20], log-logistic modified Weibull-PS [21], power inverted Topp-Leone- PS [22] distributions, among others.

Numerous writers have highlighted the significance and usefulness of inverted distributions in many fields, including engineering, economics, and medicine. In this work, the inverse power Lomax (IPL) distribution with three parameters, which was recently presented by Hassan and Abd-Allah [23], attracts our attention. The probability density function (PDF) and the cumulative distribution function (CDF) of the IPL distribution, having $\alpha,\beta>0,$ as shape parameters, and its scale parameter $\lambda>0,$ is defined, respectively, as follows:

$$g(x)=\frac{\alpha\beta}{\lambda}x^{-(\beta+1)}\left(1+\frac{x^{-\beta}}{\lambda}\right)^{-(\alpha+1)}; \qquad x>0, \tag{1}$$

and,

$$G(x)=\left(1+\frac{x^{-\beta}}{\lambda}\right)^{-\alpha}; \qquad x>0. \tag{2}$$

Due to the IPL distribution's non-monotonic failure rate, it offers greater flexibility, making it more appropriate for various practical data modeling and analytic applications. Hassan and Abd-Allah [23] looked at a few statistical characteristics and provided estimators of the parameters in censored samples. Shi and Shi [24] studied how to statistically estimate parameters of the IPL distribution when employing progressive first-failure censoring. The inference of the IEL distribution based on generalized order statistics was discussed by Nassr et al. [25].

This paper's primary objective is to create a novel asymmetric compound class of distributions that is produced by combining the IPL and PS distributions to analyze a system with parallel components; this system is known as the inverse power Lomax power series (IPLPS). We are introducing this class due to the following:

- To design several distinct models with different symmetric and asymmetric density and hazard rate functions (HRFs) shapes.
- To go over a few of its statistical characteristics, including moments, quantile function (QF), conditional moments, uncertainty measures, inverse moments, and probability-weighted moments (PWMs).

- To estimate the IPLPS class of distribution parameters, some estimation techniques are taken into consideration, such as weighted least squares (WLS), maximum likelihood (ML), Cramér von Mises (CM), and least squares (LS).
- To evaluate the effectiveness of various estimates using specific metrics, a dedicated simulation study is conducted for one special model, namely the IPL Poisson (IPLP) distribution.
- The IPLP distribution, as a sub-model within this class, demonstrates superiority over certain other distributions, as revealed through an analysis of two real-data applications.

This paper's contents are arranged as follows. The IPLPS distributions are introduced in Section 2. Many structural properties of the class are provided in Section 3. Section 4 provides certain examples of the suggested distributions. Parameter estimators for the IPLPS class using different classical methods are shown in Section 5, while Section 6 provides simulation studies. Section 7 presents the application of the suggested distribution's particular case, whereas Section 8 offers concluding findings.

2. Construction of the IPLPS Class

The IPLPS class is introduced in this section. This class of distributions is motivated by a key assumption that renders it suitable for application in each survival and reliability study. Specifically, it assumes that a device's failure arises from the presence of an unspecified number of initial faults, denoted as N, of the same type. These faults remain undetected until they lead to failure and are subsequently fixed.

If we consider X_i, i=1,…,N to represent the time until device failure caused by the ith defect supposing that these X_i's are independent and identically distributed (iid) IPL random variables, independent of N, then a truncated PS random variable, a distribution within the IPLPS class, can be utilized to model the time until the last failure. This proposed class of distributions can effectively model systems with parallel components, as many biological and industrial applications frequently do. Currently, let us explore a parallel of N iid random variables from the IPL distribution, denoted as X_i, where i=1,…,N.

Assuming that X=max $\{X_i\}_{i=1}^{N}$ be iid breakdown times of N items connected at a parallel structure, then the conditional CDF of $X\mid N$ is introduced as:

$$F_{X|N=n}(x)=\left[G(x)\right]^n=\left(1+\frac{x-\beta}{\lambda}\right)^{-\alpha n},$$

where $G(.)$ is the CDF (2) of the IPL distribution. The joint CDF is given as follows:

$$P(X\le x,N=n)=P(N=n)F_{X|N=n}(x)=\frac{a_n\theta^n}{C(\theta)}\left(1+\frac{x-\beta}{\lambda}\right)^{-\alpha n}.$$

Hence, the IPLPS class is represented by the marginal CDF of X, which takes the form:

$$F(x;\psi)=\sum_{n=1}^{\infty}\frac{a_n\theta^n}{C(\theta)}\left(1+\frac{x-\beta}{\lambda}\right)^{-\alpha n}=\frac{1}{C(\theta)}C\left(\theta\left(1+\frac{x-\beta}{\lambda}\right)^{-\alpha}\right), \tag{3}$$

where, $\psi\equiv(\alpha,\beta,\lambda,\theta)$ denotes the set of parameters, $\lambda,\theta>0$, represent scale parameters and, $\beta,\alpha>0$ indicate shape parameters. Another simplified form for (3) is as follows:

$$F(x;\psi)=\frac{1}{C(\theta)}C\left[k(x;\psi)\right];\qquad x>0, \tag{4}$$

where, $k(x;\psi)=\theta\left(1+\frac{x^{-\beta}}{\lambda}\right)^{-\alpha}$. Also, the PDF of the IPLPS class of distributions can be introduced by:

$$f(x;\psi)=\frac{\alpha\beta\theta}{\lambda C(\theta)}x^{-\beta-1}\left(1+\frac{x^{-\beta}}{\lambda}\right)^{-\alpha-1}C'\left[k(x;\psi)\right]; \qquad x>0. \tag{5}$$

The survival function and HRF associated to the IPLPS distribution are expressed as follows, respectively:

$$\bar{F}(x;\psi)=1-\frac{C\left[k(x;\psi)\right]}{C(\theta)},$$

and,

$$h(x;\psi)=\frac{\alpha\beta\theta x^{-\beta-1}C'\left[k(x;\psi)\right]}{\lambda\left[C(\theta)-C\left[k(x;\psi)\right]\right]}\left(1+\frac{x^{-\beta}}{\lambda}\right)^{-\alpha-1}.$$

Proposition: When θ approaches zero, the IPL distribution appears as a limiting special case of the IPLPS distributions

Proof: If θ approaches zero, then

$$\lim_{\theta\to0^+}F(x;\psi)=\frac{\left[\left(1+\frac{x^{-\beta}}{\lambda}\right)^{-\alpha}\right]+a_1^{-1}\lim\limits_{\theta\to0^+}\sum\limits_{n=2}^{\infty}na_n\theta^{n-1}\left[\left(1+\frac{x^{-\beta}}{\lambda}\right)^{-\alpha}\right]^{n-1}}{1+a_1^{-1}\lim\limits_{\theta\to0^+}\sum\limits_{n=2}^{\infty}na_n\theta^{n-1}}=\left(1+\frac{x^{-\beta}}{\lambda}\right)^{-\alpha},$$

which represents the CDF (2) of the IPL distribution.

Lemma 1: For the IPLPS class of distributions, the density function can be expressed as an infinite mixture of IPL distributions with parameters $(n\alpha,\beta,\lambda)$,

$$f(x;\psi)=\sum_{n=1}^{\infty}P(N=n)g(x;n\alpha,\beta,\lambda).$$

Proof: The following is an alternative form for the PDF given in Equation (5):

$$\begin{aligned}f(x;\psi)&=\sum_{n=1}^{\infty}\frac{n\alpha\beta\theta^{n}a_n x^{-(\beta+1)}}{\lambda C(\theta)}\left(1+\frac{x^{-\beta}}{\lambda}\right)^{-(\alpha n+1)}\\&=\sum_{n=1}^{\infty}P(N=n)g(x;n\alpha,\beta,\lambda),\end{aligned} \tag{6}$$

where, $g(x;n\alpha,\beta,\lambda)$ refers to the IPL distribution's density function (1) with parameters $(n\alpha,\beta,\lambda)$.

3. Some Statistical Properties

Here, several distinct statistical features of the IPLPS distributions are derived, which may include the quantile function, rth moment and inverse moment, PWMs, conditional moments, and entropy measures.

3.1 Quantile Function

The QF of the IPLPS class of X, denoted by $x_u=Q(u)=F^{-1}(u)$, is represented as follows:

$$x_u = \left\{ \lambda \left[\left(\frac{C^{-1}[uC(\theta)]}{\theta} \right)^{-1/\alpha} - 1 \right] \right\}^{-1/\beta}. \tag{7}$$

Particularly, the median, denoted by m, of the IPLPS distribution, is derived by letting $u = 0.5$ in Equation (7).

3.2 Moments and Inverse Moments

Most important properties for any distribution are concluded using ordinary moments. The rth moment of X can be introduced by using Equation (6) as follows:

$$\mu'_r = \sum_{n=1}^{\infty} P(N=n) \int_0^{\infty} \frac{n\alpha\beta}{\lambda} x^{r-(\beta+1)} \left(1 + \frac{x^{-\beta}}{\lambda}\right)^{-(\alpha n+1)} dx.$$

After simplification, the rth moment of the IPLPS distribution, can be written as:

$$\mu'_r = \sum_{n=1}^{\infty} n\alpha\lambda^{\frac{-r}{\beta}} P(N=n) \mathrm{B}\left(1 - \frac{r}{\beta}, \alpha n + \frac{r}{\beta}\right), \quad \beta > r, \quad r = 1, 2, \ldots \tag{8}$$

where, B(.,.) denotes the beta function. For r=1 in Equation (8), the mean of the IPLPS distribution is given. Also, we can get the IPLPS moment generating function from the moments by the following equation:

$$M_X(t) = \sum_{r=0}^{\infty} \frac{t^r}{r!} \mu'_r = \sum_{r=0}^{\infty} \sum_{n=1}^{\infty} \frac{n\alpha\lambda^{\frac{-r}{\beta}} t^r}{r!} P(N=n) \mathrm{B}\left(1 - \frac{r}{\beta}, \alpha n + \frac{r}{\beta}\right).$$

Furthermore, the rth inverse moment for the IPLPS distribution is derived using Equation (6) which leads to:

$$\delta_r = \sum_{n=1}^{\infty} n\alpha\lambda^{\frac{r}{\beta}} P(N=n) \mathrm{B}\left(1 + \frac{r}{\beta}, \alpha n - \frac{r}{\beta}\right), \quad r = 1, 2, \ldots$$

3.3 Conditional Moments

Studying the conditional moments is very important in lifetime models. The conditional moments of the IPLPS distribution, defined by $E\left(X^r \mid X > t\right)$, can be introduced by the following lemma.

Lemma 3.1: Supposing that X has the IPLPS $(x;\psi)$, the rth conditional moment of X, is obtained such that:

$$M_r = \sum_{n=1}^{\infty} \frac{n\alpha P(N=n)}{\lambda^{r/\beta} \bar{F}(t;\psi)} B\left(1 - \frac{r}{\beta}, \alpha n + \frac{r}{\beta}, \left(1 + \frac{t^{\beta}}{\lambda}\right)^{-1}\right),$$

where B(.,.) refers to the incomplete beta function.

Proof: Since

$$M_r = E\left(X^r \mid X > t\right) = \frac{1}{\bar{F}(t;\psi)} \int_t^{\infty} x^r f(x;\psi) dx.$$

Hence, by inserting the PDF (4) in M_r then

$$M_r = \sum_{n=1}^{\infty} \frac{n\alpha\beta P(N=n)}{\lambda \bar{F}(t;\psi)} \int_t^{\infty} x^{r-\beta-1} \left(1+\frac{x^{-\beta}}{\lambda}\right)^{-(\alpha n+1)} dx.$$

By simplifying, then the rth conditional moment of the IPLPS class of distributions can be rewritten as,

$$M_r = \sum_{n=1}^{\infty} \frac{n\alpha P(N=n)}{\lambda^{r/\beta} \bar{F}(t;\psi)} \int_0^{\left(1+t^{\beta}/\lambda\right)^{-1}} (1-z)^{\frac{-r}{\beta}} z^{\alpha n+\frac{r}{\beta}-1} dz = \sum_{n=1}^{\infty} \frac{n\alpha P(N=n)}{\lambda^{r/\beta} \bar{F}(t;\psi)} \mathrm{B}\left(1-\frac{r}{\beta}, \alpha n+\frac{r}{\beta}, \left(1+\frac{t^{\beta}}{\lambda}\right)^{-1}\right),$$

where $B(.,., x)$ is the incomplete beta function and $\bar{F}(x;\psi)$ represents the IPLPS survival function.

3.4 Probability-Weighted Moments

Greenwood et al. [26] were the first to propose the PWM approach, with the main goal being the derivation of quantiles and parameter estimators for several generalized distributions that are only analytically represented in reverse form. Eventually, for a random variable X, the PWM is expressed by the following equation:

$$\phi_{s,r} = E[X^s F(x)^r] = \int_{-\infty}^{\infty} x^s f(x) \left(F(x)\right)^r dx. \tag{9}$$

Substituting Equations (4) and (5) in Equation (9) we get:

$$\phi_{s,r} = \int_0^{\infty} x^s \frac{\alpha\beta\theta}{\lambda} x^{-\beta-1} \left(1+\frac{x^{-\beta}}{\lambda}\right)^{-\alpha-1} \frac{C'\left[k(x;\psi)\right]}{\left\{C(\theta)\right\}^{r+1}} \left(C\left[k(x;\psi)\right]\right)^r dx. \tag{10}$$

An expansion for $\left(C\left[k(x;\psi)\right]\right)^r$ can be written as follows:

$$\begin{aligned}\left[C\left(k(x;\psi)\right)\right]^r &= \left\{\sum_{n=1}^{\infty} a_n \left[k(x;\psi)\right]^n\right\}^r = (a_1)^r \left(k(x;\psi)\right)^r \\ &\times \left\{1+\frac{a_2}{a_1}\left[k(x;\psi)\right]+\frac{a_3}{a_1}\left[k(x;\psi)\right]^2+\ldots\right\}^r \\ &= \left[a_1 k(x;\psi)\right]^r \left\{\sum_{m=0}^{\infty} c_m \left[k(x;\psi)\right]^m\right\}^r, \qquad c_m = \frac{a_{m+1}}{a_1}, m=1,2,3,\ldots\end{aligned} \tag{11}$$

After that, using the Gradshteyn and Ryzhik [27] relation, which states that; for any positive integer m, the following expansion, for a positive integer r, is used:

$$\left(\sum_{m=0}^{\infty} c_m w^m\right)^r = \sum_{m=0}^{\infty} d_{r,m} w^m, \tag{12}$$

where $d_{r,0}=1$, $t \geq 1$ and the coefficients $d_{r,t} = t^{-1} \sum_{m=1}^{t} (m(r+1)-t) c_m d_{r,t-m}$. Then, using expansion (12) in (11) provides the following:

$$\left[C\left(k(x;\psi)\right)\right]^r = a_1^r \sum_{m=0}^{\infty} d_{r,m} \left[k(x;\psi)\right]^{m+r}. \tag{13}$$

In addition,

$$C'\left[k(x;\psi)\right] = \sum_{n=1}^{\infty} n a_n \left[k(x;\psi)\right]^{n-1}. \tag{14}$$

Assuming that $z = n-1$, then Equation (14) is rewritten in this form:

$$C'\left[k(x;\psi)\right] = a_1 \sum_{z=0}^{\infty} b_z (z+1)\left[k(x;\psi)\right]^z, \; b_z = \frac{a_{z+1}}{a_1}. \tag{15}$$

Hence, the PWM of the IPLPS class of distributions is represented by placing Equations (13) and (15) into (10) and after some simplification,

$$\phi_{s,r} = \frac{\alpha\beta\theta^{r+m+z+1}}{\lambda\{C(\theta)\}^{r+1}} \sum_{m,z=0}^{\infty} a_1{}^{r+1} d_{r,m} b_z (z+1) \int_0^{\infty} x^{s-\beta-1}\left(1+\frac{x^{-\beta}}{\lambda}\right)^{-\alpha(r+m+z+1)-1} dx.$$

Hence,

$$\phi_{s,r} = \sum_{m,z=0}^{\infty} A^* B\left(1-\frac{s}{\beta}, \alpha(r+m+z+1)+\frac{s}{\beta}\right), s<\beta.$$

where, $A^* = \dfrac{\alpha\theta^{r+m+z+1} a_1{}^{r+1} d_{r,m} b_z (z+1)\lambda^{\frac{-s}{\beta}}}{\{C(\theta)\}^{r+1}}$, and $B(.,.)$ is the beta function.

3.6 Entropy Measures

Entropy serves as a metric for quantifying the uncertainty within data and finds applications across diverse fields such as science, physics, and engineering. Essentially, higher entropy values indicate greater uncertainty within the data. In this sub-section, expressions for certain entropy measures within the IPLPS class are derived. Let X refers to random variable drawn from IPLPS distributions, so the Rényi entropy (RE) can be represented by the following equation:

$$I_R = \frac{1}{\delta-1}\log\left[\int_0^{\infty} f^{\delta}(x;\psi)dx\right], \delta \neq 1, \delta > 0. \tag{16}$$

Suppose $IP = \int_0^{\infty} \left(f(x;\psi)\right)^{\delta} dx$, then by using PDF (5) and expansion (14) in integral IP, we have

$$IP = \frac{(\alpha\beta\theta)^{\delta}}{\{\lambda C(\theta)\}^{\delta}} \int_0^{\infty} x^{-\delta(\beta+1)}\left(1+\frac{x^{-\beta}}{\lambda}\right)^{-\delta(\alpha+1)}\left[\sum_{n=1}^{\infty} n a_n \left[k(x;\psi)\right]^{n-1}\right]^{\delta} dx, \tag{17}$$

But $\left[\sum_{n=1}^{\infty} n a_n \left[k(x;\psi)\right]^{n-1}\right]^{\delta} = a_1^{\delta}\left[\sum_{m=0}^{\infty} c^{\bullet}_m \left[k(x;\psi)\right]^m\right]^{\delta}$, $\quad c^{\bullet}_m = \dfrac{a_{m+1}}{a_1}(m+1),\; m = 1,2,..$

According to Ref. [27], the previous equation can be expressed as:

$$\left[\sum_{n=1}^{\infty} n a_n \left[k(x;\psi)\right]^{n-1}\right]^{\delta} = a_1^{\delta} \sum_{m=0}^{\infty} d_{\delta,m}\left[k(x;\psi)\right]^m. \tag{18}$$

By using Equation (18) in the last term in (17), then

$$IP = \sum_{m=0}^{\infty} \Lambda_m B\left(\frac{\delta(\beta+1)-1}{\beta}, \delta\alpha + \alpha m + \delta - \frac{\delta(\beta+1)-1}{\beta}\right),$$
$$\Lambda_m = \frac{(\alpha\theta a_1)^{\delta}\beta^{\delta-1} d_{\delta,m}\theta^m \lambda^{\frac{\delta-1}{\beta}}}{(C(\theta))^{\delta}}. \tag{19}$$

Hence, by substituting (19) in Equation (16), the RE of the IPLPS class of distributions takes the following form:

$$I_R(\delta)=\frac{1}{1-\delta}\log\left[\sum_{m=0}^{\infty}\Lambda_m B\left(\frac{\delta(\beta+1)-1}{\beta},\delta\alpha+\alpha m+\delta-\frac{\delta(\beta+1)-1}{\beta}\right)\right].$$

Tsallis entropy (TE), introduced by Tsallis [28] as a thermodynamic measure, has a wide application across various real-world domains. Generally, TE offers intriguing explanations in physical, chemical, and biological phenomena. The TE measure is represented as:

$$I_{TE}=\frac{1}{\delta-1}\left[1-\int_0^{\infty} f^{\delta}(x)dx\right],\delta\neq 1,\delta>0.$$

Using the similar procedure discussed above, the TE is given by:

$$I_{TE}=\frac{1}{\delta-1}\left[1-\left(\sum_{m=0}^{\infty}\Lambda_m B\left(\frac{\delta(\beta+1)-1}{\beta},\delta(\alpha+1)+\alpha m-\frac{\delta(\beta+1)-1}{\beta}\right)\right)\right].$$

4. Special Sub-Models

Here, certain special cases of this class are introduced. Graphs depicting the PDF and HRF are presented to showcase the IPLP distribution' flexibility for some chosen values for the parameters.

- If $\beta=1$, the IPLPS class offers the inverse Lomax PS class of distributions (new-class).
- Letting $C(\theta)=e^{\theta}-1$, the IPLPS distribution turns to the IPLP distribution.
- Supposing that $\beta=1$, $C(\theta)=e^{\theta}-1$ and the IPLPS distribution provides the IL Poisson (ILP) distribution (new).
- Setting $C(\theta)=-\log(1-\theta)$, the IPLPS class becomes the IPL logarithmic (IPLL) distribution (new).
- By putting $\beta=1$, and $C(\theta)=-\log(1-\theta)$, the IPLPS distribution provides the IL logarithmic (ILL) distribution (Buzaridah et al. [29]).
- Considering that $C(\theta)=\theta(1-\theta)^{-1}$, the IPLPS distribution introduces the IPL geometric (IPLG) distribution (new).
- By letting $\beta=1$, and $C(\theta)=\theta(1-\theta)^{-1}$, the IPLPS distribution presents the IL geometric (ILG) distribution (new).
- Substituting $C(\theta)=(1-\theta)^{m}-1$, that yields the IPL binomial (IPLB) distribution (new).
- Taking $\beta=1$, besides $C(\theta)=(1-\theta)^{m}-1$, it gives the IL binomial (ILB) distribution.

The IPLP Distribution

By setting $C(\theta)=e^{\theta}-1$, and $C'(\theta)=e^{\theta}$ in (4) and (5), the PDF and CDF of the IPLP distribution is obtained by:

$$f_1(x;\psi)=\frac{\alpha\beta\theta}{\lambda\left(e^{\theta}-1\right)}x^{-\beta-1}\left(1+\frac{x^{-\beta}}{\lambda}\right)^{-\alpha-1}e^{k(x;\psi)};\quad x>0,$$

$$F_1(x;\psi)=\frac{e^{k(x;\psi)}-1}{e^{\theta}-1};\quad x>0,$$

where, α,β denote the shape parameters and θ,λ refer to the scale parameters. The HRF of the IPLP distribution is given as follows:

$$H_1(x;\psi)=\frac{\alpha\beta\theta x^{-\beta-1}e^{k(x;\psi)}}{\lambda\left[e^{\theta}-e^{k(x;\psi)}\right]}\left(1+\frac{x^{-\beta}}{\lambda}\right)^{-\alpha-1};x>0.$$

The PDF and HRF plots for the IPLP distribution are given in Figure 1.

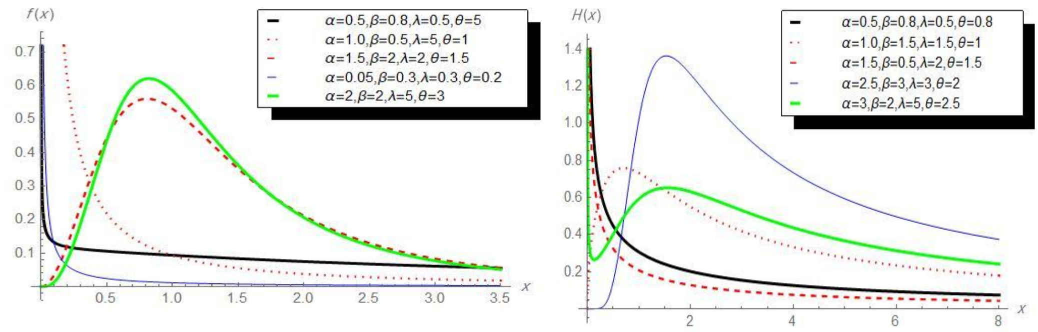

Figure 1: *PDF and HRF plots for specific parameter values of the IPLP distribution.*

Figure 1 indicates that the IPLP distribution's density may exhibit reversed-J, skewed to the right, or unimodal shapes. Moreover, the HRF can take on increasing, decreasing, upside down, or reversed J-shaped forms at different parameter values. This suggests that the IPLP distribution is versatile for fitting datasets with diverse shapes.

5. Parameter Estimation

Here, the parameter estimation for the IPLPS distributions is discussed by applying the ML, LS, WLS, and CM methods.

5.1 Maximum Likelihood Estimators

Let $x_1, x_2, \ldots, x_n$ be a simple random sample from the IPLPS class of distributions with a set of parameters $\psi = (\alpha, \beta, \lambda, \theta)^T$. The likelihood function of this sample, denoted by L_n based on the observed random sample of size n from density (5) is given by:

$$L_n = \left(\frac{\alpha\beta\theta}{\lambda C(\theta)}\right)^n \prod_{i=1}^{n} x_i^{-\beta-1}\left(1+\frac{x^{-\beta}}{\lambda}\right)^{-\alpha-1} C'\big(k(x_i;\psi)\big).$$

The log-likelihood, say $\log L_n$, , can be expressed as:

$$\log L_n = n\log(\alpha\beta\theta) - n\log(\lambda C(\theta)) - \sum_{i=1}^{n}(\beta+1)\log x_i - (\alpha+1)\sum_{i=1}^{n}\log\left(1+\frac{x_i^{-\beta}}{\lambda}\right) + \sum_{i=1}^{n}\log\big(C'(k(x_i;\psi))\big), \quad (20)$$

Hence, by differentiating (20) with respect to α, β, λ and θ, respectively, yields

$$\frac{\partial \log L_n}{\partial \alpha} = \frac{n}{\alpha} - \sum_{i=1}^{n}\log\left(1+\frac{x_i^{-\beta}}{\lambda}\right) - \sum_{i=1}^{n}\frac{\theta C''(k(x_i;\psi))}{C'(k(x_i;\psi))}\left(1+\frac{x_i^{-\beta}}{\lambda}\right)^{-\alpha}\log\left(1+\frac{x_i^{-\beta}}{\lambda}\right),$$

$$\frac{\partial \log L_n}{\partial \beta} = \frac{n}{\beta} - \sum_{i=1}^{n}\log x_i - \sum_{i=1}^{n}\frac{(\alpha+1)x_i^{-\beta}\log x_i}{\lambda + x_i^{-\beta}} + \sum_{i=1}^{n}\frac{\alpha\theta x_i^{-\beta}\log x_i C''(k(x_i;\psi))}{\lambda C'(k(x_i;\psi))}\left(1+\frac{x_i^{-\beta}}{\lambda}\right)^{-\alpha-1},$$

$$\frac{\partial \log L_n}{\partial \lambda} = -\frac{n}{\lambda} + (\alpha+1)\sum_{i=1}^{n}\frac{x_i^{-\beta}}{\lambda^2 + \lambda x_i^{-\beta}} + \sum_{i=1}^{n}\frac{\theta\alpha C''(k(x_i;\psi))}{\lambda^2 C'(k(x_i;\psi))}\left(1+\frac{x_i^{-\beta}}{\lambda}\right)^{-\alpha-1},$$

and,

$$\frac{\partial \log L_n}{\partial \theta} = \frac{n}{\theta} - \frac{nC'(\theta)}{C(\theta)} + \sum_{i=1}^{n} \frac{C''\left(k(x_i;\psi)\right)}{C'\left(k(x_i;\psi)\right)} \left(1 + \frac{x_i^{-\beta}}{\lambda}\right)^{-\alpha}.$$

Then the ML estimates (MLEs) for the parameters α, β, λ and θ, denoted by $\hat{\alpha}, \hat{\beta}, \hat{\lambda}$ and $\hat{\theta}$, can be derived by setting $(\partial L_n/\partial \alpha), (\partial L_n/\partial \beta), (\partial L_n/\partial \lambda)$ and $(\partial L_n/\partial \theta)$ to be zero and solving these equations numerically.

5.2 Least Squares and Weighted Least Squares Estimators

Consider $x_{(1)}, x_{(2)}, \ldots, x_{(n)}$ refers to an observed ordered sample and $x_1, x_2, \ldots, x_n$ represents n random samples from the IPLPS distribution. Johnson et al. [30] claimed that the distribution's expectation and variance are determined independently of the unknown parameter by

$$E\left(F(X_{(i)})\right) = \frac{i}{n+1}, \text{ and, } Var\left(F(X_{(i)})\right) = \frac{i(n-i+1)}{(n+1)^2(n+2)},$$

where $F(X_{(i)})$ indicates the CDF of any given distribution and $X_{(i)}$ denotes the statistic of order i. So, the LS estimates (LSEs) and WLS estimates (WLSEs) can be given by the minimization of the sum of all squared errors

$$H(\psi) = \sum_{i=1}^{n} v_i \left[F(x_{(i)};\psi) - E\left(F(x_{(i)};\psi)\right)\right]^2.$$

The LSEs and WLSEs of α, β, λ and θ, are produced by the minimization of the preceding function

$$H(\psi) = \sum_{i=1}^{n} v_i \left[\left(\frac{C\left[k(x_{(i)};\psi)\right]}{C(\theta)}\right) - \frac{i}{n+1}\right]^2. \tag{21}$$

Based on Equation (21), the LSEs $\hat{\alpha}_1, \hat{\beta}_1, \hat{\lambda}_1$ and $\hat{\theta}_1$ are provided by using $v_i = 1$, while the WLSE $\hat{\alpha}_2, \hat{\beta}_2, \hat{\lambda}_2$ and $\hat{\theta}_2$ are obtained by putting $v_i = \dfrac{(n+1)^2(n+2)}{i(n-i+1)}$.

These estimates can be given by solving each of the following equations numerically.

$$\frac{\partial H(\psi)}{\partial \alpha} = \sum_{i=1}^{n} v_i \left[\frac{C\left(k(x_{(i)};\psi)\right)}{C(\theta)} - \frac{i}{n+1}\right] \varphi_1\left(x_{(i)},\psi\right) = 0,$$

$$\frac{\partial H(\psi)}{\partial \beta} = \sum_{i=1}^{n} v_i \left[\frac{C\left(k(x_{(i)};\psi)\right)}{C(\theta)} - \frac{i}{n+1}\right] \varphi_2\left(x_{(i)},\psi\right) = 0,$$

$$\frac{\partial H(\psi)}{\partial \lambda} = \sum_{i=1}^{n} v_i \left[\frac{C\left(k(x_{(i)};\psi)\right)}{C(\theta)} - \frac{i}{n+1}\right] \varphi_3\left(x_{(i)},\psi\right) = 0,$$

$$\frac{\partial H(\psi)}{\partial \theta} = \sum_{i=1}^{n} v_i \left[\frac{C\left(k(x_{(i)};\psi)\right)}{C(\theta)} - \frac{i}{n+1}\right] \varphi_4\left(x_{(i)},\psi\right) = 0,$$

where,

$$\varphi_1(x_{(i)},\psi) = -\frac{\theta}{C(\theta)} \left(1 + \frac{x_{(i)}^{-\beta}}{\lambda}\right)^{-\alpha} \log\left(1 + \frac{x_{(i)}^{-\beta}}{\lambda}\right) C'(x_{(i)},\psi),$$

$$\varphi_2(x_{(i)},\psi) = \frac{\alpha\theta}{\lambda C(\theta)} \left(1 + \frac{x_{(i)}^{-\beta}}{\lambda}\right)^{-\alpha-1} x_{(i)}^{-\beta} \ln x_{(i)} C'(x_{(i)},\psi),$$

$$\varphi_3(x_{(i)},\psi)=\frac{\alpha\theta x_{(i)}^{-\beta}}{\lambda^2 C(\theta)}\left(1+\frac{x_{(i)}^{-\beta}}{\lambda}\right)^{-\alpha-1}C'(x_{(i)},\psi),$$

and,

$$\varphi_4(x_{(i)},\psi)=\frac{C'\left(k(x;\psi)\right)}{C'(\theta)}\left(1+\frac{x_{(i)}^{-\beta}}{\lambda}\right)^{-\alpha}-\frac{C\left(k\left(x_{(i)},\psi\right)\right)C'(\theta)}{\left(C'(\theta)\right)^2}.$$

5.3 Cramèr –von-Mises Estimators

This method can be defined as a type of estimator that relies on minimal distance principles since it relies on the disparity between the empirical distribution function and the CDF estimate. According to Macdonald [31], in this method, the CM estimator`s are presented as the minimization of the given equation with respect to $\alpha,\beta,\lambda,$ and θ, respectively,

$$H(\psi)=\frac{1}{12n}+\sum_{i=1}^{n}\left[\frac{C\left(k(x_{(i)},\psi)\right)}{C(\theta)}-\frac{2i-1}{2n}\right]^2.$$

The CM estimates (CMEs) $\hat{\alpha}_3,\hat{\beta}_3,\hat{\lambda}_3,$ and $\hat{\theta}_3$ can be obtained by differentiating the previous equation with respect to $\alpha,\beta,\lambda,\ \theta$, respectively, and equating it to zero.

6. Simulation Study

For each estimation problem, the investigation of the estimator's properties is very important. Analytical study of the obtained expressions for the estimators can't be effective due to their complexity. As a result, a numerical study will be established, handling the estimates' sampling distribution independently. This estimation is conducted in order to assess the estimators presented at the preceding section. All calculations are produced by using the *Mathematica11.3 program*. The performances of the different estimates will be compared according to their absolute bias (AB) and mean squared error (MSE). These numerical procedures will be shown by steps below:

Step 1: 1000 random samples given the sizes of 50, 100, 150, and 200 are conducted from the inverse power Lomax Poisson distribution.
Step 2: Four cases of parameter values have been selected such that:
Case 1 $\equiv(\alpha=0.2,\beta=0.5,\lambda=0.5,\theta=0.5)$, Case 2 $\equiv(\alpha=0.1,\beta=0.7,\lambda=0.5,\theta=0.5)$,
Case 3 $\equiv(\alpha=0.35,\beta=0.75,\lambda=0.5,\theta=0.5)$, Case 4 $\equiv(\alpha=0.7,\beta=0.25,\lambda=0.5,\theta=0.5)$.
Step 3: The MLEs, LSEs, WLSEs, and CMEs are derived for each unknown parameter.
Step 4: The ABs and MSEs of different estimates of unknown parameters are calculated. The results are written down in Tables A.1 to A.4 (Appendix A). By the help of these tables, the following conclusions can be concluded to predict the performance for all these different estimates

- For fixed value of $\lambda=0.5$ and $\theta=0.5$, ABs and MSEs for each α estimates and β estimate values in the MLEs decrease while sample size increases (see Table A.1).
- For fixed values of λ and θ, the MSEs of CMEs for α and β are decreasing and the sample size will be increasing in the same time (see Table A.3).
- For $\beta=0.75$, and for fixed values of λ and θ, the MSEs of the WLSEs increase as the sample size increases (see Table A.2).
- By increasing the sample size, the ABs of MLEs at $\alpha=0.35$ and $\beta=0.75$ decrease consistently, for fixed values for λ and θ as shown in Table A.3.

- At $n = 50$ and $\lambda = 0.5$, the MSEs have the smallest values for all different sets of parameters at $\alpha = 0.35$ and $\beta = 0.75$, as indicated in Table A.4.
- As the sample size increases, it is evident through all estimation methods that both MSEs and ABs decrease, as demonstrated in Table A.1 for instance.
- Almost in all cases, the estimated MSEs of the MLEs are the smallest compared to other estimation methods across all parameter values.

7. Data Analysis

This section presents the application of the IPLP model on two real data sets, illustrating its practical adaptability and utility. The IPLP distribution is contrasted with alternative models including the power Lomax (PL) [32], PL Poisson (PLP) [33], Topp-Leone Lomax (TLLO) [34], and Marshall Olkins PL (MOPL) [35] distributions for two real datasets.

The first dataset has been introduced by Murthy et al. [36], represents 84 observations recording the failure time for specific aircraft windshield model. The dataset is as follows:

0.04	1.866	2.385	3.443	0.301	1.876	2.481	3.467	0.309	1.899
2.61	3.478	0.557	1.911	2.625	4.57	1.652	2.3	3.344	4.602
1.757	3.578	0.943	1.912	2.632	3.595	1.07	1.914	2.646	3.699
1.124	1.981	2.661	3.779	1.248	2.01	2.224	3.117	4.485	1.652
2.229	3.166	2.688	3.924	1.281	2.038	2.823	4.035	1.281	2.085
2.89	4.121	1.303	2.089	2.902	4.167	1.432	4.376	1.615	2.223
3.114	4.449	1.619	2.097	2.934	4.24	1.48	2.135	2.962	4.255
1.505	2.154	2.964	4.278	1.506	2.19	3	4.305	1.568	2.194
3.103	2.324	3.376	4.663						

To examine the utility of the proposed models, various criteria measures, including -2Log-likelihood (L*), Akaike information criterion (A*), Bayesian information criterion (B*), consistent Akaike information criterion (C*), the Kolmogorov-Smirnov distance (K*) and its p-value (K*-PV), and CM statistics (W*) are evaluated. In general, the smaller the value of these statistics, a better fit model for the data will be found. Table 1 offers MLEs for all models that are suggested, and Table 2 lists several goodness of fitting metrics.

Table 1: *MLEs for all parameters of the models fitted to first dataset*

Model	$\hat{\alpha}$	$\hat{\beta}$	$\hat{\lambda}$	$\hat{\theta}$
IPLP	0.1987	4.4769	0.011	3.9019
PL	22.4127	2.3992	270.085	____
PLP	121.997	1.6083	332.485	3.1412
TLLO	3.7045	4.1343	0.1044	____
MOPL	*7.5277*	*1.417*	7.5784	18.0908

Table 2: *Statistical metrics for all models according to the first dataset*

Model	L*	A*	B*	C*	K*	W*	K*-PV
IPLP	310.726	318.726	319.232	328.449	0.06679	0.05164	0.823436
PL	524.280	530.279	530.579	537.572	0.0717773	0.06906	0.752356
PLP	544.968	552.968	553.475	562.692	0.0713355	0.05521	0.758912
TLLO	464.11	470.11	470.41	477.403	0.132497	0.38564	0.095490
MOPL	616.978	624.978	625.484	634.701	0.0706109	0.05595	0.769575

Table 2 clearly indicates that among all the models fitted, the IPLP model exhibits the lowest values for statistical measures. Hence, it could be regarded as the best model. Figure 2 illustrates non-parametric plots for the first dataset, encompassing total time on test (TTT), box plot, and percentile-percentile (PP) plots. Furthermore, Figure 3 presents the estimated cumulative and density functions for the fitted models.

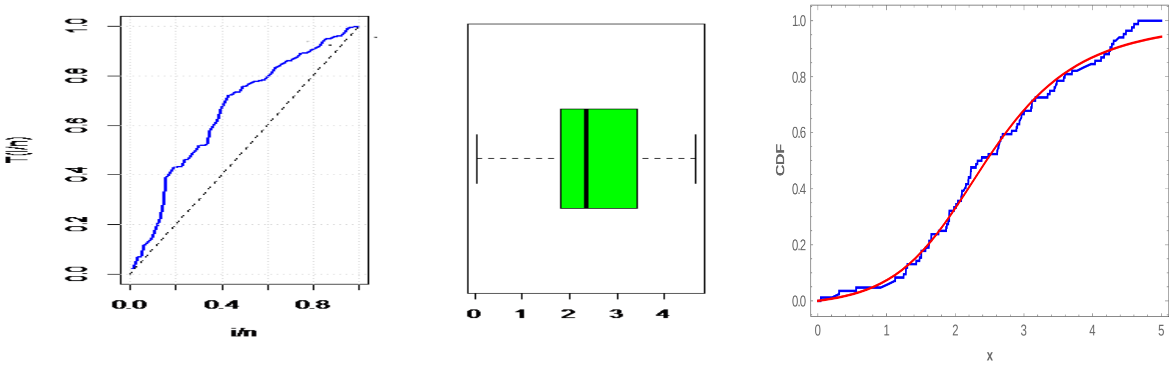

Figure 2: *The TTT plot, Box plot, and PP-plot for first data*

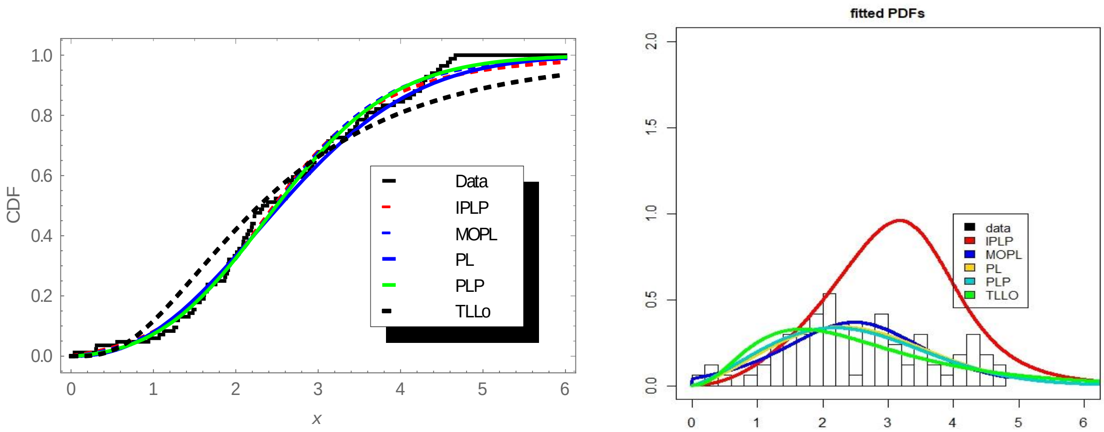

Figure 3: *Estimated CDF and PDF for the models fitted to the first dataset*.

Depending on Figure 3, the IPLP distribution provides the closest fit to the provided data, and then it is the best model among the other models to analyze these data.

Data 2: This dataset represents 63 aircraft windshield service times, presented by Murthy et al. [36]. The data can be shown as follows:

0.046	1.436	2.592	0.14	1.492	2.6	0.15	1.58	2.67	0.248
1.719	2.717	0.28	1.794	2.819	0.313	1.915	2.82	0.389	1.92
2.878	0.487	1.963	2.95	0.622	1.978	3.003	0.9	2.053	3.102
0.952	2.065	3.304	0.996	2.117	3.483	1.003	2.137	3.5	1.01
2.141	3.622	1.085	2.163	3.665	1.092	2.183	3.695	1.152	2.24
4.015	1.183	2.341	4.628	1.244	2.435	4.806	1.249	2.464	4.881
1.262	2.543	5.14							

Table 3 lists the MLEs for all models that are suggested, while Table 4 gives the numerical values of the statistical metrics.

Table 3: *MLEs for the unknown parameters of the models fitted to the second dataset*

Model	$\hat{\alpha}$	$\hat{\beta}$	$\hat{\lambda}$	$\hat{\theta}$
IPLP	0.2238	3.8211	0.0233	2.0577
PL	108.647	1.6327	422.985	______
PLP	131.468	1.3335	256.861	1.8047
TLLO	1.9449	4.5615	0.0834	______
MOPL	0.7228	3.1157	0.0161	69.0443

Table 4: *Statistical metrics for the proposed models according to the second dataset*

Model	L*	A*	B*	C*	K*	W*	K*-PV
IPLP	536.838	544.839	545.529	553.411	0.0684147	0.056686	0.909991
PL	633.596	639.596	640.002	646.025	0.109307	0.0945244	0.409648
PLP	545.928	553.928	554.617	562.5	0.0898046	0.0571536	0.656499
TLLO	569.62	575.62	576.026	582.049	0.145844	0.273631	0.123926
MOPL	542.74	550.74	551.429	559.312	0.137781	0.204885	0.166429

Results in Table 4 show the utility of the IPLP model as it has the lowest L*, A*, B*, C*, K*, and W* values and has the greatest K*-PV compared to the others, which indicates that the IPLP distribution is the best model. In addition, Figures 4 and 5 give TTT Plot, box plot, and PP-plot, along with the estimated cumulative and densities of the fitted models plot as well, respectively, for the data.

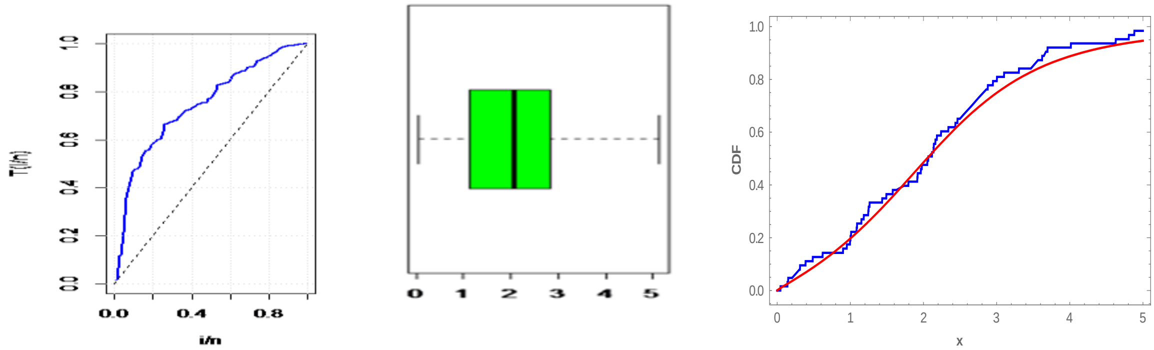

Figure 4: *The TTT plot, box plot and PP-plot for second data*

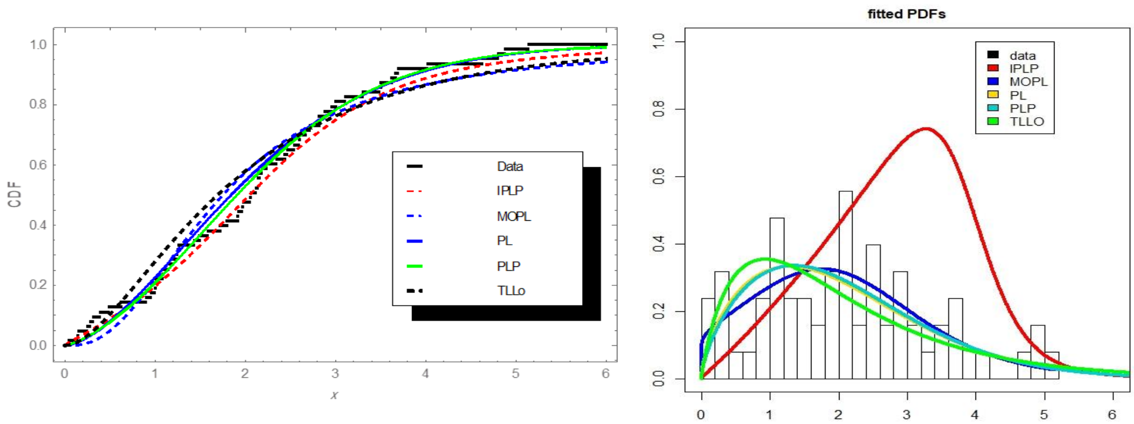

Figure 5: *The estimated CDF and PDF for the models fitted to the second dataset*

Figure 5 demonstrates that the IPLP distribution closely aligns with the histogram, indicating its superiority over other models for analyzing this data.

8. Concluding Remarks

A novel asymmetric four-parameter IPLPS class of distributions formed by combining the inverse power Lomax and power series distributions is introduced in this paper. This blending technique enables the creation of adaptable distributions with significant implications across diverse fields such as engineering and biology. The IPLPS class includes a new compound class and many novel compound distributions, which come as new sub-models. Expressions for the QF, conditional moments, inverse moments, PWMs, and uncertainty measures are constructed. Estimation of model parameters is carried out using WLS, ML, CVM, and LS techniques. We assess and compare several parameter estimators for the IPLP distribution using an in-depth simulation study. Additionally, we demonstrate the efficacy of the proposed model using two real datasets, where it exhibits superior fit compared to alternative models.

Appendix A: Tables

Table A.1: *Results of simulation study of different estimates for the IPLP distribution: Case 1*

Case 1 $(\alpha = 0.2, \beta = 0.5, \lambda = 0.5, \theta = 0.5)$						
n	Method	Measure	α	β	λ	θ
50	ML	AB	0.006745	0.077041	0.029852	0.115995
		MSE	0.007617	0.041746	0.120200	0.197901
	LS	AB	0.430544	0.487070	0.144346	0.113605
		MSE	0.269951	0.238003	0.140357	0.146791
	WLS	AB	0.288091	0.441809	0.096579	0.384180
		MSE	0.149819	0.215351	0.123369	0.789747
	CM	AB	0.339837	0.487085	0.131450	0.304000
		MSE	0.174023	0.238043	0.114371	0.620196
100	ML	AB	0.000455	0.057409	0.001818	0.076642
		MSE	0.004357	0.023858	0.083599	0.185695
		SE	0.000066	0.000143	0.000289	0.000424
	LS	AB	0.447667	0.491493	0.156331	0.123996
		MSE	0.281292	0.241848	0.137407	0.143057
		SE	0.000284	0.000017	0.000336	0.000357
	WLS	AB	0.279684	0.461081	0.073950	0.399205
		MSE	0.145609	0.221363	0.119117	0.831226
		SE	0.000259	0.000094	0.000337	0.000819
	CM	AB	0.334056	0.493331	0.132073	0.361127
		MSE	0.162428	0.243538	0.102497	0.692470
150	ML	AB	0.000429	0.034402	0.004477	0.047673
		MSE	0.002593	0.013023	0.065901	0.178032
		SE	0.000051	0.000109	0.000257	0.000419
	LS	AB	0.444868	0.494006	0.155821	0.116442
		MSE	0.270110	0.244186	0.128611	0.130407
	WLS	AB	0.296139	0.462616	0.085070	0.348997
		MSE	0.152255	0.222201	0.115882	0.733505
	CM	AB	0.343748	0.493717	0.146006	0.373102
		MSE	0.166483	0.244084	0.097878	0.750284
200	ML	AB	0.001551	0.023436	0.012966	0.031401
		MSE	0.002002	0.009062	0.056420	0.170785
	LS	AB	0.452990	0.494879	0.168071	0.114122
		MSE	0.275720	0.244991	0.131350	0.134244
	WLS	AB	0.300224	0.468995	0.087634	0.360930
		MSE	0.155801	0.226458	0.117244	0.801838
	CM	AB	0.338092	0.495897	0.128463	0.359770
		MSE	0.163050	0.245969	0.094788	0.693901

Table A.2: *Results of simulation study of different estimates for the IPLP distribution: Case 2*

Case 2 $(\alpha = 0.1, \beta = 0.7, \lambda = 0.5, \theta = 0.5)$						
n	Method	Measure	α	β	λ	θ
50	ML	AB	0.002242	0.091436	0.052315	0.088154
		MSE	0.001661	0.047267	0.112424	0.190250
	LS	AB	0.514374	0.688831	0.134479	0.098571
		MSE	0.348814	0.475298	0.140524	0.136474
	WLS	AB	0.382270	0.650093	0.080623	0.348311
		MSE	0.215249	0.443329	0.119549	0.738434
	CM	AB	0.408666	0.690469	0.107712	0.382826
		MSE	0.221501	0.477186	0.104083	0.756821
100	ML	AB	0.000734	0.064783	0.027290	0.064352
		MSE	0.000925	0.032769	0.087944	0.176691
	LS	AB	0.549471	0.692815	0.168821	0.119962
		MSE	0.383591	0.480338	0.142214	0.142375
	WLS	AB	0.356645	0.660133	0.060534	0.444925
		MSE	0.191185	0.447833	0.117684	0.891369
	CM	AB	0.425101	0.694151	0.110837	0.335976
		MSE	0.234942	0.481978	0.100780	0.717249
150	ML	AB	0.001048	0.047594	0.030172	0.060538
		MSE	0.000739	0.026150	0.076517	0.168294
	LS	AB	0.548601	0.694918	0.164571	0.123721
		MSE	0.378798	0.483023	0.138253	0.138424
	WLS	AB	0.363182	0.662171	0.067058	0.387271
		MSE	0.191053	0.449580	0.114219	0.801316
	CM	AB	0.433434	0.695742	0.138198	0.388423
		MSE	0.236302	0.484116	0.098432	0.783373
200	ML	AB	0.000355	0.035961	0.024822	0.018055
		MSE	0.000581	0.021184	0.065165	0.162195
	LS	AB	0.557505	0.695863	0.168104	0.133845
		MSE	0.390652	0.484309	0.138774	0.144132
	WLS	AB	0.358781	0.670564	0.063388	0.438549
		MSE	0.190053	0.454457	0.111519	0.828456
	CM	AB	0.421589	0.696359	0.125404	0.424671
		MSE	0.228737	0.484958	0.102214	0.859722

Table A.3: *Results of simulation study of different estimates for the IPLP distribution: Case 3*

Case 3 $(\alpha=0.35, \beta=0.75, \lambda=0.5, \theta=0.5)$						
n	Method	Measure	α	β	λ	θ
50	ML	AB	0.028882	0.038793	0.041519	0.097016
		MSE	0.021385	0.024007	0.093766	0.205833
	LS	AB	0.330981	0.720645	0.172635	0.214191
		MSE	0.200888	0.522177	0.156952	0.153552
	WLS	AB	0.171788	0.664002	0.111915	0.315342
		MSE	0.094188	0.468671	0.125394	0.676175
	CM	AB	0.200807	0.723881	0.139624	0.297306
		MSE	0.094502	0.526193	0.108873	0.592616
100	ML	AB	0.011510	0.032625	0.034154	0.045939
		MSE	0.010988	0.017202	0.073926	0.191679
	LS	AB	0.343760	0.730998	0.176993	0.239639
		MSE	0.204578	0.535951	0.150556	0.161608
	WLS	AB	0.183232	0.681750	0.121003	0.315958
		MSE	0.096159	0.485995	0.114875	0.638105
	CM	AB	0.196654	0.733830	0.131675	0.316076
		MSE	0.088577	0.539333	0.100398	0.589016
150	ML	AB	0.009429	0.021253	0.021613	0.045372
		MSE	0.008488	0.012985	0.061332	0.185365
	LS	AB	0.347205	0.736845	0.183141	0.228068
		MSE	0.198331	0.543845	0.142716	0.156601
	WLS	AB	0.158364	0.678758	0.094665	0.387196
		MSE	0.091379	0.481589	0.118032	0.745790
	CM	AB	0.197847	0.737241	0.133215	0.322106
		MSE	0.088204	0.544097	0.096084	0.576261
200	ML	AB	0.005265	0.018039	0.032937	0.005198
		MSE	0.005849	0.010298	0.052733	0.183501
	LS	AB	0.330284	0.738295	0.161452	0.216034
		MSE	0.183964	0.545553	0.130130	0.155453
	WLS	AB	0.181529	0.692042	0.112438	0.315812
		MSE	0.096914	0.492804	0.114267	0.617612
	CM	AB	0.185704	0.739790	0.125346	0.377463
		MSE	0.083501	0.541593	0.094968	0.691230

Table A.4: *Results of simulation study of different estimates for the IPLP distribution: Case 4*

Case 4 $(\alpha=0.7, \beta=0.25, \lambda=0.5, \theta=0.5)$						
n	Method	Measure	α	β	λ	θ
50	ML	AB	0.002412	0.026550	0.017636	0.062220
		MSE	0.056895	0.005150	0.097176	0.176375
	LS	AB	0.004458	0.236684	0.175355	0.196397
		MSE	0.090972	0.056577	0.154987	0.154997
	WLS	AB	0.118599	0.213013	0.132290	0.293232
		MSE	0.095884	0.049828	0.129123	0.667014
	CM	AB	0.100852	0.237882	0.168351	0.251028
		MSE	0.074475	0.057127	0.116832	0.562473
100	ML	AB	0.011686	0.012692	0.031510	0.009029
		MSE	0.396155	0.002067	0.076041	0.170751
	LS	AB	0.019738	0.241765	0.204124	0.214818
		MSE	0.087939	0.058649	0.158975	0.161972
	WLS	AB	0.115818	0.222881	0.142248	0.273083
		MSE	0.085862	0.051960	0.121264	0.574088
	CM	AB	0.131302	0.241384	0.149405	0.309364
		MSE	0.070562	0.058503	0.105365	0.588599
150	ML	AB	0.019717	0.005788	0.035701	0.010170
		MSE	0.030271	0.001102	0.058667	0.153535
	LS	AB	0.012704	0.244189	0.198267	0.207426
		MSE	0.082305	0.059729	0.150544	0.160624
	WLS	AB	0.114129	0.224038	0.144723	0.293595
		MSE	0.086913	0.052262	0.124999	0.661949
	CM	AB	0.133418	0.243985	0.142315	0.290336
		MSE	0.070266	0.059684	0.103061	0.557025
200	ML	AB	0.012894	0.005315	0.039573	0.030536
		MSE	0.025921	0.000908	0.053184	0.153984
	LS	AB	0.027965	0.245094	0.218293	0.217001
		MSE	0.078031	0.060166	0.152014	0.158960
	WLS	AB	0.103315	0.226621	0.161816	0.278613
		MSE	0.085451	0.052928	0.130257	0.629098
	CM	AB	0.117752	0.244956	0.169220	0.286765
		MSE	0.064152	0.060075	0.104847	0.525627

References

[1] Barreto-Souza, W., de Morais, A. L., and Cordeiro, G. M. (2011). The Weibull-geometric distribution. *Journal of Statistical Computation and Simulation*, 81(5):645–657.

[2] Noack, A. (1950). A class of random variables with discrete distributions. *The Annals of Mathematical Statistics*, 21(1):127–132.

[3] Chahkandi, M., and Ganjali, M. (2009). On some lifetime distributions with decreasing failure rate, *Computational Statistics and Data Analysis*, 53:4433–4440

[4] Morais, A. L., and Barreto-Souza, W., (2011). A compound class of Weibull and power series distributions. *Computational Statistics and Data Analysis*, 55:1410–1425.

[5] Warahena-Liyanage, G., and Pararai, M. (2015). The Lindley power series class of distributions: model, properties and applications. *Journal of Computations & Modelling*, 5(3): 35–80.

[6] Elbatal, I., Zayed, M., Rasekhi, M., and Butt, N. (2017). The exponential Pareto power series distribution: *Theory and applications. Pakistan Journal of Statistics and Operation Research*, 13(3): 603–615, https://doi.org/10.18187/pjsor.v13i3.2072

[7] Silva, R. B. and Cordeiro, G. M. (2015). The Burr XII power series distributions: A new compounding family. *Brazilian Journal of Probability and Statistics*, 29(3): 565–589

[8] Alizadeh, M., Bagheri, S. F., Samani, E. B., Ghobadi, S., and Nadarajah, S. (2018). Exponentiated power Lindley power series class of distributions: Theory and applications. *Communications in Statistics-Simulation and Computation*, 47(9):2499–2531.https://doi.org/10.1080/03610918.2017 .1350270

[9] Elbatal, I., Altun, E., Afify, A. Z., and Ozel, G. (2018). The generalized Burr XII power series distributions with properties and applications. *Annals of Data Science*, 6:571–597 https://doi.org/10.1007/s40745-018-0171-2.

[10] Goldoust, M., Rezaei, S., Alizadeh, M., Nadarajah, S. (2019). The odd log-logistic power series family of distributions: Properties and applications. *Statistica*, 79(1):77–107. https://doi.org/10.6092/issn.1973-2201/8115

[11] Kunjiratanachot, N., Bodhisuwan, W. and Volodin, A. (2018). The Topp-Leone generalized exponential power series distribution with applications. *Journal of Probability and Statistical Science*, 16(2): 197–208.

[12] Hassan, A. S., and Assar, S. M. (2021). A new class of power function distribution: Properties and applications. *Annals of Data Science*, 8: 205–225, https://doi.org/10.1007/s40745-019-00195-7

[13] Rivera, P. A., Calder´ın-Ojeda, E., Gallardo, D. I., and G´omez, H. W. (2021). A compound class of the inverse gamma and power series distributions. *Symmetry*, 13, 1328.

[14] Hassan, A. S., Almetwally, E. M, Gamoura, S. C, Metwally, A. S. M. (2022). Inverse exponentiated Lomax power series distribution: Model, estimation, and application. *Journal of Mathematics*, 2022, 1998653, https://doi.org/10.1155/2022/1998653

[15] Khojastehbakht, N., Ghatari, A., and Samani, E. B. (2023). The beta exponential power series distribution. *Annals of Data Science*, 10(5):1157–1178, https://doi.org/10.1007/s40745-022-00414-8

[16] Alghamdi, S. M., Shrahili, M., Hassan, A. S., Mohamed, R.E., Elbatal, I., and Elgarhy, M. (2023). Analysis of milk Production and failure data: Using unit exponentiated half logistic power series class of distributions. *Symmetry*, 15, 714, https://doi.org/10.3390/sym15030714

[17] Ul-Haq, M, A., Shahzad, M, K., and Tariq, S. (2023). The inverted Nadarajah–Haghighi power series distributions. International *Journal of Applied and Computational Mathematics*,10(11), https://doi.org/10.1007/s40819-023-01551-1.

[18] Hassan, A. S., and Abd-Allah, M., (2023). Power quasi-Lindley power series class of distributions: Theory and applications. *Thailand Statistician*, 21(2): 314–336

[19] Zayed, M. A., Hassan, A. S., Almetwally, E. M., Aboalkhair, A. M., Al-Nefaie, A. H., and Almonry, H. M. (2023). A compound class of unit Burr XII model: Theory, estimation, fuzzy, and application. *Scientific Programming*, https://doi.org/10.1155/2023/4509889

[20] Yousef, M. M., Hassan, A. S., and Almetwally, E. M. (2024). Statistical inference for the unit Gompertz power series distribution using ranked set sampling with applications. *Assiut University Journal of Multidisciplinary Scientific Research*, 53(1):154–189.

[21] Oluyede, B., Dingalo, N. and Chipepa, F. (2024). A new and generalized class of log-logistic modified Weibull power series distributions with applications. *Thailand Statistician* 22(2), 237–273

[22] El-Saeed, A.R., Hassan, A.S., Elharoun, N.M., Al Mutairi, A., Khashab, R.H., Nassr, S.G. (2023). A class of power inverted Topp-Leone distribution: Properties, different estimation methods & applications. *Journal of Radiation Research and Applied Sciences*, 16 (2023) 100643, https://doi.org/10.1016/j.jrras.2023.100643

[23] Hassan, A. S., and Abd-Allah, M. (2019). On the inverse power Lomax distribution. *Annals of Data Science*, 6: 259–278, https://doi.org/10.1007/s40745-018-0183-y

[24] Shi, X., and Shi, Y. (2021). Inference for inverse power Lomax distribution with progressive first-failure censoring. *Entropy*, 23, 1099. https://doi.org/10.3390/ e23091099

[25] Nassr, S. G., Hassan, A. S., Almetwally, E. M., Al Mutairi, A., Khashab, R. H. and ElHaroun, N. M. (2023). Statistical inference of the inverted exponentiated Lomax distribution using generalized order statistics with application to COVID-19. *AIP Advances,* 13, 105118; https://doi.org/10.1063/5.0174540.

[26] Greenwood, J. A., Landwehr, J. M., Wallis, J. R., and Matals, N. C. (1979). Probability weighted moments: Definition and relation to parameters of several distributions expressable in inverse form. *Water Resources Research*, 15:1094–1054

[27] Gradshteyn, I. S.; and Ryzhik, I. M. Table of Integrals, Series and Products; Academic Press: San Diego, CA, USA, 2000.

[28] Tsallis, C. (1988). Possible generalization of Boltzmann-Gibbs statistics. *Journal of Statistical Physics*, 52(1):479–487

[29] Buzaridah, M., Ramadan, D. A, and El-Desouky, B. (2021). Flexible reduced logarithmic-inverse Lomax distribution with application for bladder cancer. *Open Journal of Modelling and Simulation*. 09(04):351–369. https://doi.org/10.4236/ojmsi.2021.94023.

[30] Johnson, N. L., Kemp, A. W., and Kotz, S. Univariate Discrete Distributions. Wiley-Interscience, third edition, 2005.

[31] MacDonald, P. D. M. (1971). Comment on "an estimation procedure for mixtures of distributions" by Choi and Bulgren. *Journal of the Royal Statistical Society. Series B (Methodological)*, 33(2): 326–329.

[32] Rady, E. A., Hassanein, W. A., and Elhaddad, T. A. (2016). The power Lomax distribution with an application to bladder cancer data, *Springer Plus,* https://www.ncbi.nlm.nih.gov/pubmed/ 27818876.

[33] Hassan, A. S., and Nassr, S. (2018). Power Lomax Poisson distribution: Properties and estimation. *Journal of Data Science*, 18, 105–128. https://doi.org/10.6339/JDS.201801_16 (1).0007

[34] Oguntunde, P., Khaleel, M., Okagbue, H., and Odetunmibi, O. (2019). The Topp–Leone Lomax (TLLo) distribution with applications to airborne communication transceiver dataset. *Wireless Personal Communications*. 109. https://doi.org/10.1007/s11277-019-06568-8.

[35] Ul Haq, M. A., Hamedani, G. G., Elgarhy, M., and Ramos, P. L. (2020). Marshall-Olkin power Lomax distribution: Properties and estimation based on complete and censored samples. International *Journal of Statistics and Probability*, *Canadian Center of Science and Education*, 9(1): 1–48.

[36] Murthy, D. N. P., Xie, M. and Jiang, R. Weibull Models. Wiley, 2004.